

On the fluctuations of jamming coverage upon random sequential adsorption on homogeneous and heterogeneous media.

Ernesto S. Loscar, Rodolfo A. Borzi and Ezequiel V. Albano^a

^a*Instituto de Investigaciones Fisicoquímicas Teóricas y Aplicadas (INIFTA), UNLP, CONICET, Suc.4, CC16, 1900 La Plata, Argentina*

October 28, 2018

Abstract

The fluctuations of the jamming coverage upon Random Sequential Adsorption (RSA) are studied using both analytical and numerical techniques. Our main result shows that these fluctuations (characterized by σ_{θ_j}) decay with the lattice size according to the power-law $\sigma_{\theta_j} \propto L^{-1/\nu}$. The exponent ν depends on the dimensionality D of the substrate and the fractal dimension of the set where the RSA process actually takes place (d_f) according to $\nu = \frac{2}{2D-d_f}$. This theoretical result is confirmed by means of extensive numerical simulations applied to the RSA of dimers on homogeneous and stochastic fractal substrates. Furthermore, our predictions are in excellent agreement with different previous numerical results.

It is also shown that, studying correlated stochastic processes, one can define various fluctuating quantities designed to capture either the underlying physics of individual processes or that of the whole system. So, subtle differences in the definitions may lead to dramatically different physical interpretations of the results. Here, this statement is demonstrated for the case of RSA of dimers on binary alloys.

1 Introduction

Physical and chemical properties of adsorbed monolayers are being studied with increasing interest because their understanding is essential for the rationalization of many phenomena and processes occurring on surfaces and interfaces, such as adsorption, desorption, catalysis, corrosion, wetting, adhesion, diffusion, etc. The equilibrium behavior of such overlayers can be described by a Gibbs measure parametrized by the coverage θ and the temperature T . Within this context, the critical behavior of adsorbed films has extensively been studied [1, 2, 3]. On the other hand, numerous physical processes can be modeled as the sequential, irreversible filling of a surface by atoms or molecules. Some examples are the reaction at specific sites on a polymer chain, adsorption onto surfaces, reaction between groups on adjacent surface sites, etc. [4, 5, 6].

Considering the irreversible deposition of particles on a surface, one has two characteristic time scales: the time between depositions, and the diffusion time of the particles on the surface. For very strong interaction between particles and the substrate (chemical adsorption), diffusion becomes irrelevant and the venerable Random Sequential Adsorption (RSA) model provides an excellent description of the underlying processes (for a review on RSA models see e.g. [6]). Under these conditions the system evolves rapidly toward far-from equilibrium conditions and the dynamics becomes essentially dominated by geometrical exclusion effects between particles. This kind of effects has been observed in numerous experiments [7].

When RSA involves adsorption on single sites, the case is termed ‘monomer filling’. Also, processes involving adjacent pairs of sites are referred as ‘dimer filling’, while adsorption on larger ensembles of sites corresponds to ‘animal filling’ [6]. A quantity of central interest for the understanding of RSA processes is the asymptotic value of the fraction θ of the total surface occupied by adsorbed objects, which is called the jamming coverage $\theta_J = \theta(t \rightarrow \infty)$. Within this context, the RSA of needles (or linear segments) on homogeneous, two-dimensional samples, has very recently attracted considerable interest [8, 9]. Particular attention has been drawn to the interplay between jamming and percolation [8, 9, 10]. Of course, the percolation problem is a topic of enormous interest by itself, due to their applications not only in statistical physics but also in many other areas such as the study of disordered media, fluids in porous materials, systems of biological and ecological interest, etc. [11, 12, 13]. , a great progress in the field of the statistical physics of far-from equilibrium processes could be achieved by establishing links between RSA and percolation [8, 9, 10].

Percolation is essentially a geometrical critical phenomena. The percolation transition is related to the probability of occurrence of an infinite connectivity between randomly deposited objects, as a function of the fraction p of the substrate occupied by the objects [14]. At the critical point (p_c), the percolation cluster in d -dimensions, is a random fractal of dimension $D_F = d - \beta/\nu$, where β and ν are the order parameter and correlation length critical exponents, respectively. Close to criticality, the probability P to find a percolating cluster, on a finite sample of side L can be described by means of an error function [13]

$$P = \frac{1}{\sqrt{2\pi}\Delta} \int_{-\infty}^p \exp\left[-\frac{1}{2}\left(\frac{p^* - p_c}{\Delta}\right)^2\right] dp^*, \quad (1)$$

where Δ is the width of the transition region. It is well known that the width vanishes in the thermodynamic limit according to [13]

$$\Delta \propto L^{-\frac{1}{\nu}}. \quad (2)$$

Eq. (2) is very useful because it allows for the measure of the correlation length exponent ν that governs the divergence of the correlation length as $\xi \propto |p - p_c|^{-\nu}$ (for random percolation with $d = 2$ one has $\nu = 4/3$).

Very recently it has been suggested that the jamming probability and the fluctuations of the jamming coverage may obey relationships similar to Eqs. (1) and (2) [8], respectively. Also, for the jamming upon RSA of needles in two dimensions the value $\nu_J = 1.0 \pm 0.1$ has been reported [8] and this figure is independent of the aspect ratio of the needles. Furthermore, early numerical results of Nakamura for the RSA of square blocks are also consistent with $\nu_J \simeq 1$ [15], while Kondrat and Pekalski [9] have reported $\nu_J = 1.00 \pm 0.05$ for the RSA of segments on the square lattice. Since the obtained values for the exponent are independent (within error bars) of: i) the length of the segments (for all $a = 1, 2, \dots, 45$) [9], ii) the aspect ratio of the needles [8] and iii) the size of the square blocks [15], it has been suggested that ν_J is a good candidate for an universal quantity of the jamming process [9].

The aim of this manuscript is to provide a qualitative derivation of Eq. (2) for the case of RSA on heterogeneous media. It is shown that the exponent ν_J can be obtained as a function of the dimensionality D of the space and the fractal dimension d_f of the subset of sites where the RSA process actually takes place. Our main result

$$\nu_J = \frac{2}{2D - d_f}, \quad (3)$$

provides a solid ground to previous numerical data [8, 9, 15]. In fact, these data were obtained in $D = 2$ and $d_f = 2$, so it follows straightforwardly from Eq. (3) that $\nu_J = 1$ exactly. Furthermore, in this work, the validity of the proposed relationship (3) is verified by means of extensive numerical simulations, using both homogeneous substrates as well as different random fractals.

2 Definitions and Approaches

When studying RSA on homogeneous samples the definition of the jamming coverage and its fluctuations is straightforward, since one has to deal with a single stochastic process. However, RSA on nonhomogeneous substrates may involve the treatment of at least two correlated stochastic processes: the selection of the particular substrate where the deposition is going to take place, and the RSA process itself. In relation with the first process we will define the *substrate system* as the set $\{A_\lambda\}$, composed of M different independent substrates labeled by the index $\lambda = 1, \dots, M$. We consider that n independent RSA processes are performed for each element A_λ of the substrate system until the jammed state is reached. We call $B_k^{(\lambda)}$ ($k = 1, \dots, n$) the n different configurations adopted by the entities adsorbed on top of the substrate. The set $\{B_k^{(\lambda)}\}$ taken for the values of k (for each and all substrate) will be referred to as the RSA system.

The jamming coverage θ_J is a relevant intensive quantity that takes the value $\theta_k^{(\lambda)}$ when evaluated over the configuration $B_k^{(\lambda)}$. Let us explicitly consider two contributions to θ_J given by

$$\theta_J = \theta_{\{sub\}} + \delta\theta_{\{Rsa\}}, \quad (4)$$

It is also assumed that the first term gives the most important contribution to θ_J , that can be evaluated according to

$$\theta^{(\lambda)} = \sum_{k=1}^n \frac{\theta_k^{(\lambda)}}{n}. \quad (5)$$

Then, the fluctuations of this term are given by

$$\sigma_{\{sub\}} = \sqrt{\sum_{\lambda=1}^M \frac{(\theta^{(\lambda)} - \langle\theta_J\rangle)^2}{M-1}}. \quad (6)$$

where $\langle\theta_J\rangle$ is the average value of θ_J , taken over all measurements and configurations

$$\langle\theta_J\rangle = \sum_{\lambda=1}^M \frac{\theta^{(\lambda)}}{M}. \quad (7)$$

The second term in Eq. (4) has a zero average for a fixed substrate. Some fluctuations in θ must also appear from this term and can be characterized by the following average [16]

$$\sigma_{\{Rsa\}}^2 = \sum_{\lambda=1}^M \frac{\sigma_{\theta}^{(\lambda)2}}{M}, \quad (8)$$

$\sigma_{\theta}^{(\lambda)}$ being given by

$$\sigma_{\theta}^{(\lambda)} = \sqrt{\sum_{k=1}^n \frac{(\theta_k^{(\lambda)} - \theta^{(\lambda)})^2}{n-1}} \quad (9)$$

It should be stressed that $\sigma_{\{sub\}}$ and $\sigma_{\{Rsa\}}$ account for the fluctuations on the substrate and RSA system, respectively. So, it is expected that these quantities will describe the relevant physical behavior related with both sources of randomness.

Finally, the total root mean square deviation (RMS) σ_{θ} , that is expected to describe the fluctuation of the whole system, is given by

$$\sigma_{\theta} = \sqrt{\sum_{\lambda=1, k=1}^{M, n} \frac{(\theta_k^{(\lambda)} - \langle\theta\rangle)^2}{Mn-1}} \quad (10)$$

In general, different RMS's are related. In the simplest case when both contributions in Eq. (4) are statistically independent, the total fluctuation of θ is given by

$$\sigma_\theta = \sqrt{\sigma_{\{Sub\}}^2 + \sigma_{\{Rsa\}}^2}. \quad (11)$$

As will be shown later, Eq. (11) is essential for the analysis of numerical data obtained using finite systems and their corresponding extrapolation to the thermodynamic limit, because each term may behave according to different laws. Therefore, simply measuring σ_θ , one may obtain inaccurate results, undesired crossover effects and consequently misleading physical interpretations.

Let us now evaluate the fluctuations associated with the RSA system using the definition given by Eq. (8). Let $n_i = 0, 1$ define the occupational state of the site i . $N = \sum_{i=1}^{L^D} n_i$ is the number of particles deposited in a volume $\Omega = L^D$ of a D -dimensional lattice with periodic boundary conditions. The two-point correlation function for a homogeneous substrate is given by

$$G(i, j) = \langle n_i n_j \rangle - \langle n_i \rangle \langle n_j \rangle \quad (12)$$

where i, j labels sites and $\langle \rangle$ means average taken over the RSA system in which N varies. There is a fundamental relationship between G and the fluctuation in the number of particles given by

$$\sigma_N^2 = \sum_{i,j=1}^{L^D} G(i, j). \quad (13)$$

For the case of a unique homogeneous substrate it is well known that, when the correlation length is much shorter than the size of the system, one has

$$\sigma_N^2 = g N_A. \quad (14)$$

Here $g = \sum_{j=1}^{L^D} G(i, j)$ is independent of N_A , the number of sites where RSA takes place. The fluctuation of the density (θ) in the thermodynamic limit can be obtained after dividing both sides of Eq. (14) by a L^{2D} so that

$$\sigma_{\{Rsa\}} \propto L^{-\frac{D}{2}}, \quad (15)$$

Let us now generalize this result in order to show so that it still holds for substrates having sites where deposition is forbidden. The existence of these blocked sites on the adsorbing surface breaks the translation symmetry of the substrate, which was a necessary condition in the above deduction. However, an equation analogous to Eq. (15) can still be found if we restrict ourselves to those cases where although each substrate A_λ is nonhomogeneous, the set $\{A_\lambda\}$ is homogeneous as a whole, i.e., there is no preferred sites on the average. Stated in a more quantitative way, the following calculations are valid for systems where the average of n_i over substrates is independent of i . Then, using a procedure analogous to that employed in the derivation of Eq. (8), one can generalize Eq. (13) by writing

$$\sigma_{N\{Rsa\}}^2 = \sum_{\lambda=1}^M \sum_{i,j=1}^{L^D} \frac{G_\lambda(i, j)}{M} = \sum_{i,j=1}^{L^D} \left(\sum_{\lambda=1}^M \frac{G_\lambda(i, j)}{M} \right) \quad (16)$$

where the expression within parenthesis could be a measure of correlations over the substrate system. However, for a fixed site i there may exist substrates in the adsorptive matrix where the deposition is forbidden, so that $G_\lambda(i, j) \equiv 0$ for all j . Then, since not all the M substrates would be contributing in the sum over λ , simply dividing by M one cannot obtain the real average of G over λ . In order to have a proper average of the RSA correlation function, it is necessary to introduce a factor X_i , such that $X_i M$ is the actual number of substrates with $G_\lambda(i, j) \neq 0$. It should be noticed that for systems that are homogeneous as a whole one has $X_i \equiv X$, so that

$$\sigma_{N\{Rsa\}}^2 = X \sum_{i,j=1}^{L^D} \sum_{\lambda=1}^M \frac{G_\lambda(i, j)}{MX} = X \sum_{i,j=1}^{L^D} G^*(i, j). \quad (17)$$

In order to evaluate X , the fraction of substrates where a site is not blocked, one has to count the number of non-zero terms in Eq. (16). Adding first over j one obtains

$$g_\lambda(i) = \sum_{j=1}^{L^D} G_\lambda(i, j). \quad (18)$$

Notice that this procedure implies that $g_\lambda(i) \equiv 0$ for blocked i -sites in a fixed substrate λ , while $g_\lambda(i) \neq 0$ otherwise. The remaining double sum

$$\sum_{\lambda=1, i=1}^{M, L^D} g_\lambda(i), \quad (19)$$

can be computed fixing λ and running i over the sites. Then one obtains that the number of contributing terms is exactly the number of active sites in this substrate. Therefore, the summation over λ has ML^{d_f} terms, where L^{d_f} is the average number of active sites of the lattice where RSA actually takes place.

When i is fixed and the sum given by Eq. (19) runs over λ , it yields MX_i terms (instead of M). Then the summation $\sum_{i=1}^{L^D} MX_i$ has $ML^D X_i$ terms. Comparing now both results and using again the fact that there is no preferred sites in the global system, it follows that $X = \frac{L^{d_f}}{L^D}$. It should be noticed that this correction factor is not totally unexpected. In fact, for a substrate system that is homogeneous as a whole, one expects that the fraction of substrates with a fixed site i active X_i , should equal the average proportion of active sites given by L^{d_f}/L^D .

Now, replacing X in Eq. (17), it follows

$$\sigma_{N\{Rsa\}}^2 = \frac{L^{d_f}}{L^D} \sum_{i,j=1}^{L^D} G^*(i, j). \quad (20)$$

If the substrate system is homogeneous as a whole, then G^* should be invariant under translations, because the average of G over λ should have the same symmetries than those of the substrate system. Thus, $g^*(i) = \sum_{j=1}^{L^D} G^*(i, j)$ must be site-independent (i.e., $g^*(i) = g_0^*$), and then Eq. (20) becomes

$$\sigma_{N\{Rsa\}}^2 = L^{d_f} g_0^*. \quad (21)$$

Finally, if the correlation length $\xi_{\{Rsa\}}^*$ associated with G^* for the RSA process is short enough ($\xi_{\{Rsa\}}^* \ll L$), g_0^* is L -independent. Then the fluctuation of the density (θ) can be obtained from Eq. (21) dividing by L^{2D} , so that

$$\sigma_{\{Rsa\}} \propto L^{-\frac{1}{\nu}}, \quad (22)$$

where

$$\nu = \frac{2}{2D - d_f}. \quad (23)$$

It should be stressed that Eqs. (22) and (23) are quite general relationships valid for substrate systems that are homogeneous as a whole. Furthermore, the condition that the correlation length of the RSA process should be smaller than the system size is usually valid for jammed states, where the correlation length is very short.

Eqs. (22) and (23) also holds for homogeneous substrates, with $L^{d_f} = L^D$ and $G_\lambda \equiv G$, so $\nu = \frac{2}{D}$. These equations are also valid for nonhomogeneous random substrates where the dimensionality D of the space may be different to the dimensionality of the subset of sites where the RSA process actually takes place. It is also very interesting to notice that, using these relationships it may be possible to evaluate d_f performing RSA both in numerical simulations and actual experiments. Furthermore, existing numerical simulations performed in $D = 2$ dimensions with $d_f = 2$ are in excellent agreement with Eqs. (22) and (23) (notice that for these conditions it follows straightforwardly from Eq. (23) that $\nu = 1$ exactly): i) Nakamura [15] has reported $\nu_J \simeq 1$ (RSA of square blocks), ii) Vandewalle [8] have reported $\nu_J = 1.0 \pm 0.1$ (RSA of needles), and iii) Kondrat and Pekalski [9] have reported $\nu_J = 1.00 \pm 0.05$ (RSA of segments).

In addition to these promising results, we will provide more astringent tests of the validity of Eq. (23) performing numerical simulations of the RSA of dimers on homogeneous substrates in $D = 1, 2$ dimensions and as well as using fractal substrates.

3 Details on the Numerical Simulation of RSA of Dimers

3.1 RSA of dimers on Binary alloys

The first set of simulations are performed for the RSA of dimers (the RSA system being the adsorbed atoms) on a binary alloy (**BA**) annealed at a given temperature (substrate system). The **BA** is simulated using the isomorphism with the Ising model [17], namely spin-up $\equiv A$ -species and spin-down $\equiv B$ -species. The square lattice of side L in $D = 1, 2$ dimensions with nearest-neighbor (NN) interactions will be considered. The **BA** is in contact with a thermal bath at temperature T . The system is assumed to obey Kawasaki dynamics [17], so that the density of species A and B is conserved with $\rho_A = \rho_B = 1/2$.

The Hamiltonian (H) is given by

$$H = E_0 - J \sum_{\langle i,j \rangle} s_i s_j \quad (24)$$

where $E_0 = N(\epsilon_{AA} + \epsilon_{BB} + 2\epsilon_{AB})$, $J = -(1/4)(\epsilon_{AA} + \epsilon_{BB} - 2\epsilon_{AB})$, ϵ_{XY} is the interaction energy between X - and Y -species, and $s_i = \pm 1$ indicates A, B sites so that $\sum_i s_i = 0$ [18]. The Monte Carlo time step (MCS) involves L^D trials, such that each species of the sample is selected once on average. Stationary configurations of the **BA** are obtained after disregarding 10^5 MCS. It is well known that for $D = 1$ the system is not critical, exhibiting a (trivially) ordered phase only for $T = 0$. However, in $D = 2$ dimensions the system undergoes an order-disorder transition at $T_c = 2.269\dots$, where T_c is the Onsager critical temperature (the temperature T is measured in units of J setting Boltzmann constant at unity). Below this transition temperature, the dynamics of the underlying Ising model can be very slow because the system gets trapped on different metastable states separated between each other by high energy barriers. In order to have meaningful and systematic results, we have taken the same initial configuration for the simulation of each low temperature substrate ($T < T_c$). The starting configuration chosen was the one with lowest energy, in which A - and B -species are segregated into two identical domains, separated by non-defective (straight) domain-walls.

RSA of dimers on the **BA** is assumed to take place on top of NN sites occupied by unlike species, i.e., AB -sites, adsorption on AA - and BB -sites being forbidden. Also multiple occupation of AB -sites is forbidden. These assumptions are based on the dissociative chemisorption of diatomic molecules (O_2, H_2, N_2 , etc.) on binary catalysts. It is well known that in the absence of dimer's diffusion there is a jammed state [19], so that the relevant quantity is the jamming coverage (θ_J). In the case of homogeneous ($D = 1$) lattice one has the exact result $\theta_J = 1 - e^{-2} \simeq 0.86466472$ [6]. Also, in the homogeneous ($D = 2$) lattice one has $\theta_J \approx 0.906$ [6]. For the present case of a **BA** one expects the coverage to depend on the temperature at which the substrate has been annealed. Also, it should satisfy $\theta_J^{(AB)} \leq \theta_J$, due to the additional constraint that dimers can only be adsorbed on specific pairs of sites of the lattice.

3.2 RSA of dimers on fractal surfaces

We have also studied the RSA of dimers on stochastic fractals such as the diffusion front [11, 12] and Ising clusters [17]. It is important to stress that these chosen fractals satisfy the required property of invariance due to their stochastic nature, so that Eqs. (22) and (23) are expected to hold.

Considering a **BA** at $T = T_C$, the greatest cluster made up taking NN sites occupied by the same species, is selected for different lattice sizes. This kind of substrate, called spin clusters of the Ising model (SCIM), are fractals with a fractal dimension given by

$$d_f = D - \frac{\beta}{\nu}, \quad (25)$$

where D is the Euclidean dimension, β and ν are the order-parameter and the correlation-length critical exponents, respectively. For $D = 2$ one has $\beta = \frac{1}{8}$ and $\nu = 1$, so that $d_f = 15/8$.

In order to simulate the RSA of dimers on SCIM's, a site of the cluster is selected at random. If that site is empty, a NN site is also selected at random. The adsorption trial is successful only if that second selected site is also empty, otherwise if that site is either occupied or lies outside the fractal, the trial is disregarded. Therefore, double occupation of sites belonging to the fractal is forbidden.

RSA along the perimeter of SCIM's has also been studied. For this purpose, only adsorption events of dimers taking place on two NN sites, such as one of them belongs to the cluster and the remaining one is outside it, are considered.

Another type of stochastic fractal used for RSA simulations is that generated by a diffusion front. In fact, it is well known that the properties of the diffusion front [21, 22, 23, 24, 25] are closely related to those of the incipient percolation cluster [11, 12, 13]. The front is a (stochastic) self-similar fractal of dimension [20] $d_f^{DF} = 10/7 \approx 1.42857$ [21, 22, 23].

In order to obtain diffusion fronts suitable for RSA of dimers, we have simulated the diffusion of particles at random. Hard-core interactions, on a $D = 2$ square lattice of size $L \times L$, has been considered. There is a source of particles at the first row of the lattice $y = 1, 1 \leq x \leq L$ kept at concentration $p(y) \equiv 1$. Also, at the last row $y = L, 1 \leq x \leq L$, there is a well such as $p(L) \equiv 0$. So, there is a concentration gradient along the source-well direction, while along the perpendicular x -direction periodic boundary conditions are imposed. As the concentration $p(y)$ of particles depends on the position, decreasing from the source to the well, one actually has a **gradient percolation** system. The structure of the diffusion front is identical to the structure of the hull of the incipient percolation cluster [21, 26]. Furthermore, the concentration of particles at the mean front position y_f is the same as the percolation threshold p_c , so that $p(y_f) = p_c$ [21, 27].

Considering that particles are connected to their first neighbors while empty sites are connected to both their first and second neighbors, the system can conveniently be described by means of the following geographical analogy: The **land** is the set of particles connected to the source and the **sea** is the set of connected empty sites not surrounded by land. Also, an **island** is formed by groups of particles not connected with the land, while **lakes** are formed by connected empty sites surrounded by land. Finally, the **seashore** is the part of the land in contact with the sea that can be identified with the **diffusion front**, which is a **self-similar** fractal.

RSA of dimers on diffusion fronts has been simulated using two rules: **Rule I** is that used for the case of RSA on the SCIM perimeter (see above); while using **Rule II** one only allows the adsorption on sites of the diffusion front, disregarding adsorption trials on already occupied sites of the front and sites outside the fractal.

4 Simulation results and discussion

4.1 RSA of dimers on Binary Alloys

The simplest test for Eq. (23) corresponds to the case $D = d_f = 1$. Since for **BA** we are only allowing deposition on unlike sites, this example can be realized taking a one dimensional **BA** with nearest-neighbor repulsion between unlike species (antiferromagnetic Ising system). In fact, considering the ground state at $T = 0$, corresponding to a fully

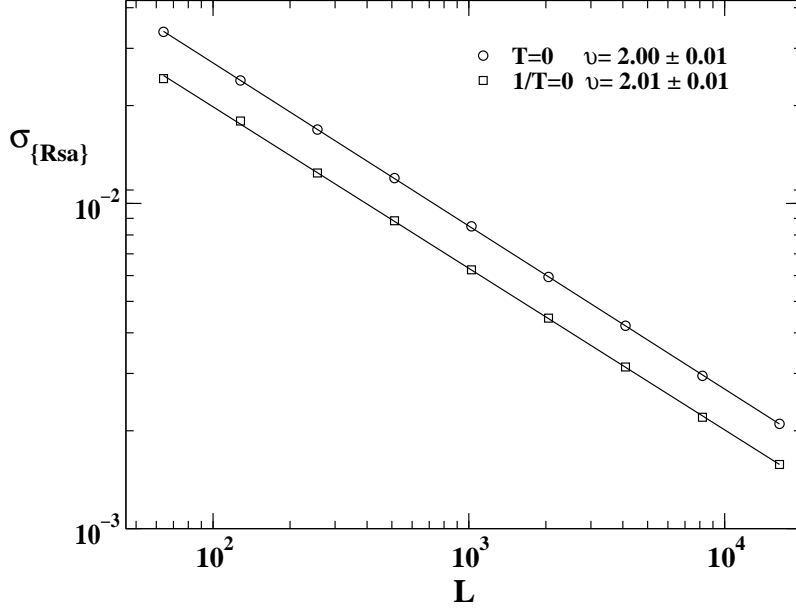


Figure 1: Log-log plots of $\sigma_{\{Rsa\}}$ versus L obtained the case of RSA on **BA**'s in 1 dimension ($D = 1$). **BA**'s at two different temperatures, $T = 0$ and $T = \infty$, are considered as shown in the figure.

ordered sample, one has that the **BA** is irrelevant and the system is equivalent to the standard RSA of dimers in $D = 1$. On the other hand, for $T > 0$ one has disordered samples with an homogeneous distribution of blocked sites, *i.e.*, *AA*- and *BB*-sites where dimers are not adsorbed. Particularly, at $T = \infty$ one has a fully disordered substrate. The obtained results are shown in Fig. 1 as log-log plots of $\sigma_{\{Rsa\}}$ versus L . The best fits of the data give $\nu = 2.00 \pm 0.01$ and $\nu = 2.01 \pm 0.01$ for the cases $T = 0$ and $T = \infty$, respectively. Both figures are in excellent agreement with the prediction of Eq. (23) for $D = d_f = 1$, namely $\nu = 2$.

The second example considered corresponds to RSA on a $D = 2$ **BA** with NN attractive interactions between alike species, *i.e.* the ferromagnetic version of the Ising model with conserved order parameter. In this case one can also tests the validity of Eq. (11) by measuring all the involved terms according to Eqs. (6), (8) and (10), respectively. Fig. 2 shows log-log plots of σ_θ versus $\sqrt{\sigma_{\{Sub\}}^2 + \sigma_{\{Rsa\}}^2}$ obtained for the case of RSA of dimers on two dimensional **BA**'s. Data was taken at different temperatures and using lattices of different size. The excellent straight line obtained, corresponding to 150 independent measurements, strongly supports the validity of Eq. (11).

Also, Fig. 3 shows plots of $\sigma_{\theta\{Rsa\}}$ versus L for the RSA of dimers on **BA**'s obtained at different temperatures. It is found that the power law decay predicted by Eq. (22) always holds allowing us to determine the exponents ν . At low temperatures, below T_c , one has that the **BA** segregates into domains of alike species containing a certain density of unlike species (impurities) trapped into the bulk, which increases when the temperature is raised. Since dimer adsorption on the bulk of the domains is not possible due to the adsorption rule that have been imposed, at very low temperatures the RSA process is essentially

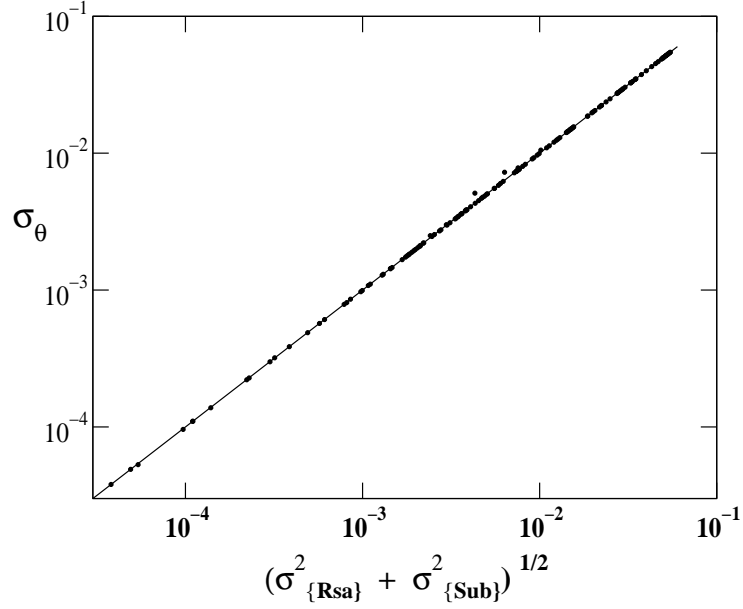


Figure 2: Log-log plots of σ_θ versus $\sqrt{\sigma_{\{Sub\}}^2 + \sigma_{\{Rsa\}}^2}$, as suggested by Eq. (11). The different terms involved in Eq. (11) were obtained according to Eqs. (6) and (8) (*horizontal axis*) and (10) (*vertical axis*), respectively. The straight line has slope unity.

restricted to the interface between domains. In this case one has $d_f = 1$ and Eq. (23) predicts $\nu = 2/3$, in excellent agreement with the results obtained fitting the curves, as shown in the inset of Fig. 3. Increasing the temperature and particularly close to T_c , the density of impurities located into the bulk of the domains increases. Consequently, an increasing number of pairs of sites becomes available for the RSA of dimers. However, not all these sites contribute to the fluctuations of the jamming coverage. The simplest example is the case of a single impurity surrounded by unlike species where only one dimer, with four possible orientations, can be adsorbed. Therefore, fluctuations of the jamming coverage are only relevant when adsorption takes place in rather complex arrangements of impurities that are present in the domains close to T_c . For these reasons one observes a smooth increase of ν when approaching the critical point from below, as shown in the inset of Fig. 3. Finally, for $T \geq T_C$ one has that adsorption sites, given by nearest-neighbor pairs of unlike species, are homogeneously distributed on the sample with $D = 2$ and $d_f = 2$. For this case, Eq. (23) predicts $\nu = 1$ in excellent agreement with the numerical results shown in the inset of Fig. 3. It should be noticed that the smooth variation of ν , observed in the inset of Fig. 3 when approaching T_c , may be due to finite-size effects that hinder the evaluation of the actual exponents. If this is the case, the exponents $2/3 < \nu_{eff} < 1$, may be considered as effective size-dependent exponents.

In order to further support the above discussed interpretation of the evaluated values of the exponent ν , numerical simulations using samples having controlled interface roughness and concentration of impurities, have been performed. The starting substrate is a ground state of the **BA** ($T = 0$) in $D = 2$. The half-left (-right) side of the sample is filled with A - (B -) species, so that a perfectly flat interface of AB -species runs along the middle of

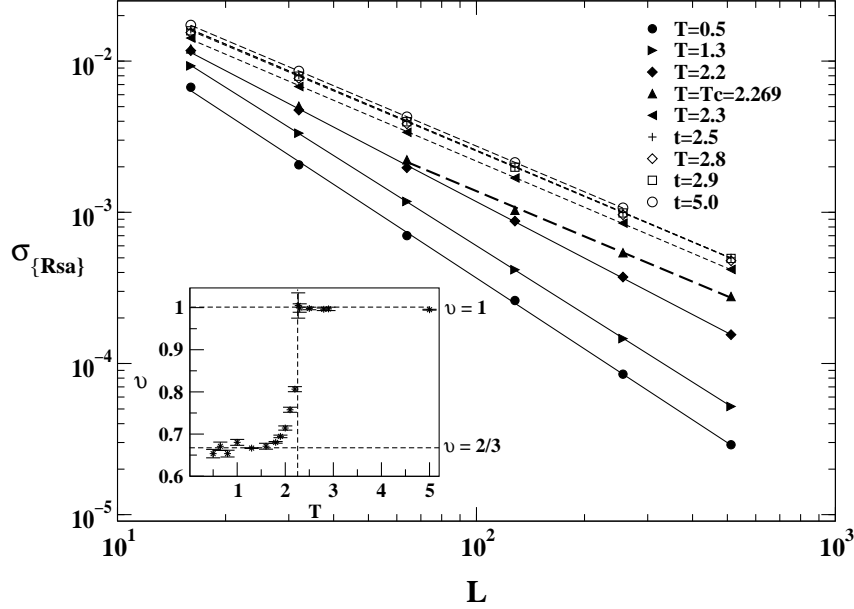


Figure 3: Log-log plots of $\sigma_{\{Rsa\}}$ versus L obtained at different temperatures performing in each case $n = 500$ and $M = 500$ measurements. The inset shows the temperature dependence of the exponent ν (temperature is measured in units of J).

the sample. Since RSA on this substrate has zero rms, the original interface is modified introducing kink-like defects with probability p_k . The resulting interface where the RSA process actually occurs is homogeneous with fractal dimension $d_f = 1$, so that according to Eq. (23) one should expect an exponent $\nu = 2/3$. This prediction is again in excellent agreement with the numerical results obtained taking $p_k = 0.005, 0.05, 0.3$ and 0.5 , as shown in Fig. 4(a). Of course, for $p_k = 0.005$ and small lattices ($L \leq 100$), finite size effects are observed due to the finite probability of having a perfectly flat interface without fluctuations.

In addition to the test described previously, samples with a fixed interface roughness ($p_k = 0.3$) in the example shown in Fig. 4(b) were decorated with a controlled density (ρ_I) of impurities uniformly distributed in the bulk of the domains. Fig. 4(b) shows that the presence of impurities not only causes the fluctuations to increase but also $\nu \rightarrow 1$ for large values of ρ_I , as expected for $D = 2$ and $d_f = 2$ according to Eq. (23). The value $\nu = 0.70 \pm 0.03$ obtained for $\rho_I = 1/8$ is very close to the figure $\nu = 2/3$ corresponding to $\rho_I = 0$ since a majority of isolated and small clusters of impurities can not significantly influence neither the fluctuations nor the exponent. In fact, only more complex clusters of impurities, as those formed for $\rho_I = 1/3$ and $\rho_I = 2/3$ in the example shown in Fig. 4(b), allow for a large variety of adsorption configurations with an appreciable enhancement of the fluctuations of the RSA process that causes a noticeable effect on the exponent.

4.2 RSA of dimers on fractal surfaces

Fig. 5 shows log-log plots of $\sigma_{\{Rsa\}}$ versus L obtained upon RSA of dimers on SCIM's. In this example one has $D = 2$ and $d_f = 15/8$, so that the value $\nu = 16/17 \simeq 0.941176$

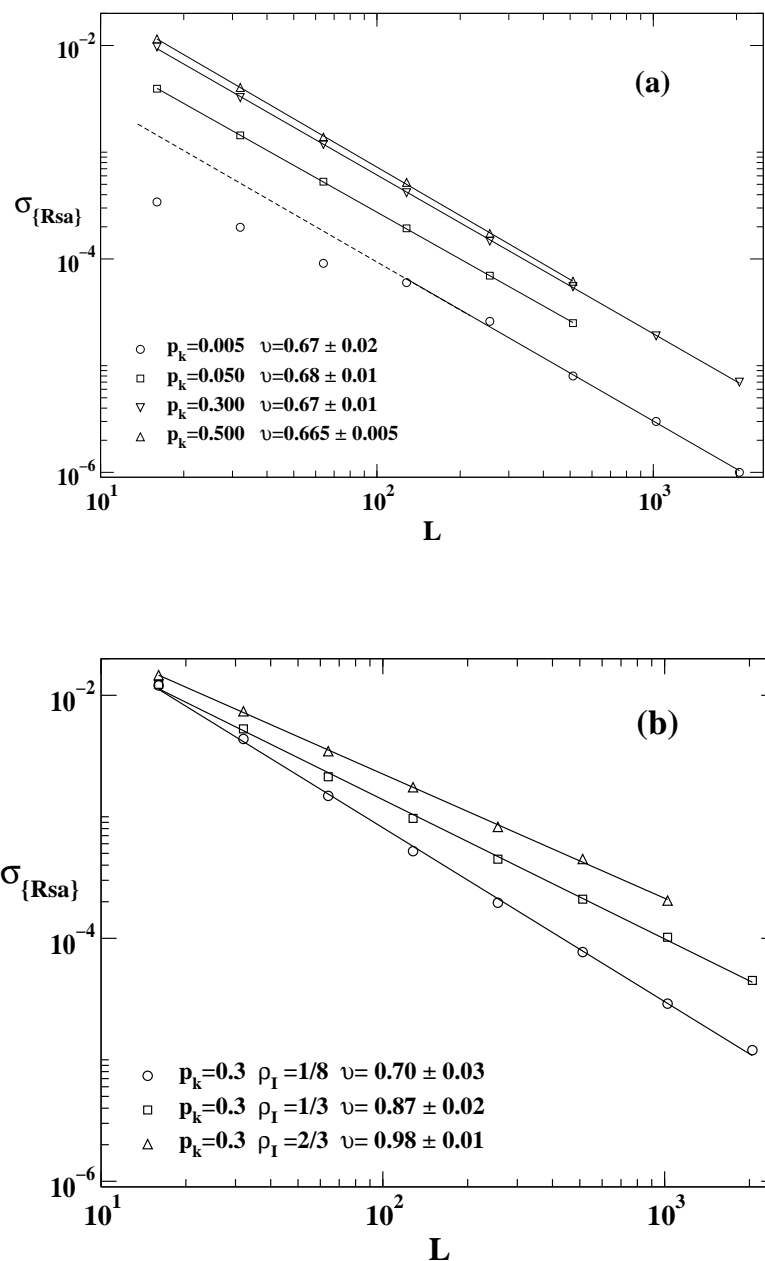


Figure 4: Log-log plots of $\sigma_{\{Rsa\}}$ versus L obtained for a simple one-dimensional interfacial model embedded in a two dimensional lattice. The parameter p_k allow us to choose different interface roughness, while ρ_I accounts for the density of two-dimensional defects in the bulk. For additional details on the model see the text. (a) Data corresponding to $\rho_I = 0$ and different values of the roughness, as listed in the figure. (b) Data obtained keeping the roughness $p_k = 0.3$ fixed and using different values of ρ_I , as listed in the figure.

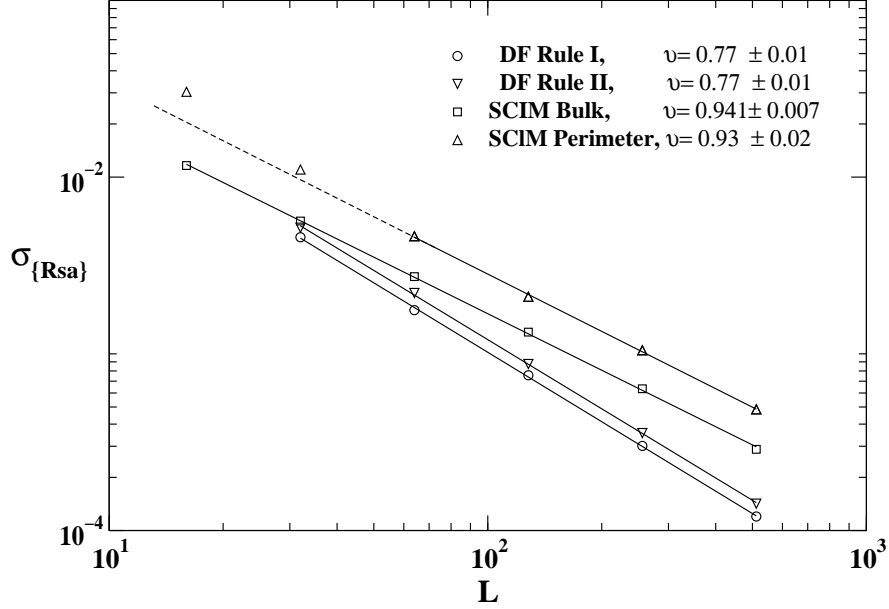


Figure 5: Log-log plots of $\sigma_{\{Rsa\}}$ versus L for the case of RSA on random fractals. Considering Spin Clusters of the Ising model (SCIM) at T_c , it is found that Eq. (23) is valid when the RSA process is done on both, the bulk and the perimeter cluster. Also, results obtained upon RSA on the fractal generated by diffusion fronts (DF) with two different adsorption rules, are shown. For details on the SCIM and the adsorption rules see the text.

is expected according to Eq. (23). The results obtained fitting the data corresponding to RSA on the bulk of the cluster and on its perimeter are $\nu = 0.941 \pm 0.007$ and $\nu = 0.93 \pm 0.02$, respectively. In the latter case for small lattices ($L \leq 60$), finite size effects are observed as in the analogous percolation problem [13]. Also, Fig. 5 shows the results for the RSA of dimers on a diffusion front in $D = 2$. This is an interesting example to test the validity of Eq. (23) using an stochastic fractal with a well known fractal dimension $d_f = 10/7$. For this example one expects $\nu = 0.777\dots$ while the best fit of the numerical data shown in Fig. 5 gives $\nu = 0.77 \pm 0.01$, using two different adsorption rules as discussed above. These results are also in excellent agreement with Eq. (23) giving further numerical support to the analytical relationship derived in Section 2.

4.3 Interplay between fluctuations of correlated stochastic processes

It should be stressed that in order to capture the physics of the RSA process, all the fluctuations measured in the previous sections were evaluated with the aid of Eqs. (8) and (9). The aim of this subsection is to show that a quite different physical picture can be obtained measuring the fluctuations linked with the substrate system. Let us recall that for this purpose one also has to perform RSA measurements, however fluctuations have to be evaluated using Eqs. (6), which within the context of the present work, captures

the physics of the underlying substrate where the RSA process takes place.

As an example, the discussion will be restricted to the case of RSA of dimers on a **BA** in $D = 2$, in order to perform comparisons with the data obtained in the simulations shown in Figs. 2 and 3. Considering a single configuration of the alloy and according to the adsorption rules, one has that θ_J is essentially a measure of the density of AB -sites present in the configuration. Furthermore, such pairs (which are known as the ‘broken bonds’ in Ising spin language), contribute to the internal energy per site of the **BA** (u). Applying the fluctuation-dissipation theorem [28] it is possible to show that the specific heat of the **BA** ($C_V = (\frac{\partial u}{\partial T})_V$) is given by the fluctuations of u , namely

$$C_V = \frac{L^2}{T^2} \sum_{\lambda=1}^M \frac{(u_\lambda - \langle u \rangle)^2}{M-1} = \frac{L^2}{T^2} \sigma_u^2 \quad (26)$$

where averages are taken over the set $\{A_\lambda\}$ of different configurations of the **BA**. On the other hand, for the $D = 2$ Ising model one has that

$$C_V(T) \propto |T - T_C|^\alpha, \quad (27)$$

with $\alpha \equiv 0$, i.e. a logarithmic divergence at criticality. Analogously, one can define an RSA ‘susceptibility’ χ for the jammed state as

$$\chi = L^2 \sum_{\lambda=1}^M \frac{(\theta_J^\lambda - \langle \theta_J \rangle)^2}{M-1} = L^2 \sigma_{\{Sub\}}^2, \quad (28)$$

where it is expected that, if the system conformed by the deposited particles would follow (or ‘copy’), in some way, the structure of the underlying substrate, χ would follow the same behavior that C_V .

Fig. (6) shows that plots of χ versus T , obtained using lattices of different size, exhibit clear peaks close to the critical temperature of the underlying **BA**, resembling the behavior of the specific heat in finite samples. In fact, the peaks are shifted and rounded due to operation of finite-size effects. This behavior is the typical one for a second-order phase transition that implies the existence of a diverging correlation length ξ when approaching criticality according to [17]

$$\xi(T) \propto |T - T_C|^{-\nu^*}, \quad (29)$$

where $\nu^* = 1$ is the correlation length exponent of the Ising model. Using finite-size scaling arguments one can set $L^{1/\nu^*} |T - T_c| \approx 1$ [17], then replacing into Eq. (27) with $\alpha = 0$, using Eq. (28) and assuming that close to criticality one has $\chi \sim C_v$, it follows

$$\chi_{max}(L) \propto \ln(L), \quad (30)$$

where χ_{max} is the maximum value of χ that can be obtained from the peaks shown in Fig. 6. The results shown in Figs. 7(a) and 7(b) confirm the divergences of χ expected according to Eqs. (27) and (30), respectively. So, this finding shows that there is an additional (divergent) correlation length of the RSA process that is associated to the substrate, and it can be captured by measuring χ .

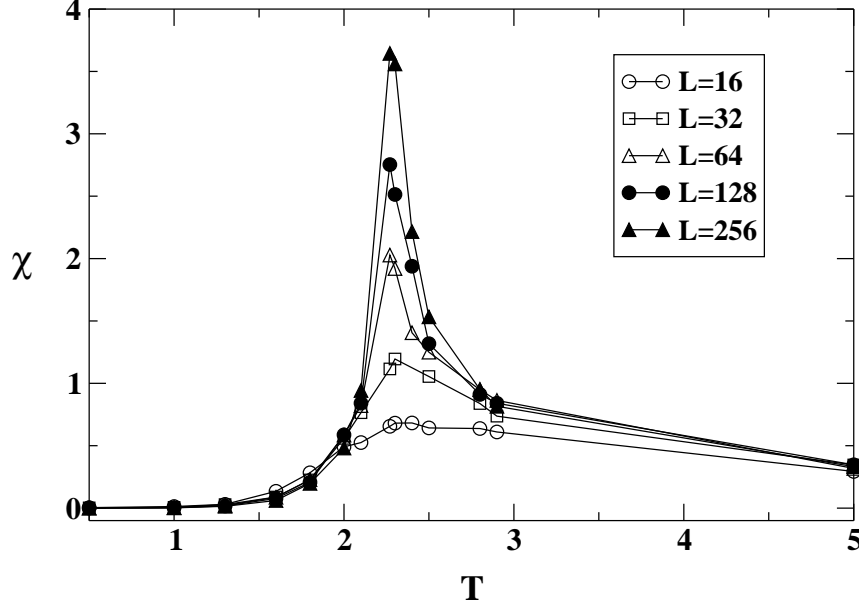


Figure 6: Plots of χ versus T obtained for the RSA of dimers on **BA** using lattices of different size L (T in units of J). The data exhibits the typical behavior characteristic of a second-order phase transition.

From Figs. 3, 6 and 7, as well as according to the above discussion, it follows that the RSA of dimers on **BA**'s provides an interesting example of the interplay between two correlated processes whose respective fluctuations obey different functions. It is worth mentioning that, in spite of exhibiting quite different behavior, both functions capture the criticality of the substrate. In fact, the fluctuations of the jammed state, as measured according to Eqs. (6) and (28), reflect the critical behavior of the **BA** through the relationship between χ and C_v while, on the other hand, using Eqs. (8) and (9) the criticality of the **BA** becomes evident through the jump of the exponent ν observed close to T_c (see Fig. 3). It is also interesting to remark that the relationship that relates the different fluctuations of both processes, given by Eq. (11), does not show such a critical behavior at all, as shown in Fig. 2.

In order to further analyze these results, let us define $\phi^* = \sigma_{\{Rsa\}}/\sigma_{\{Sub\}}$, such as ϕ^* gives a measure of the relative intensity of the RSA fluctuations as compared to those of the substrate. Then, using Eqs. (28), (22) and (30), it follows that

$$\phi^* = \phi(T)f(L) = \phi(T)\frac{L^{-1/\nu}}{L^{-1}\sqrt{\ln(L)}}, \quad (31)$$

where the L -dependence behavior of ϕ^* appears explicitly through the function $f(L)$, while $\phi(T)$ accounts for the temperature dependence. Fig. 8 shows that log-linear plots of $\phi(T) = \phi^*/f(L)$ versus T exhibit an acceptable collapsing. At both sides of T_c the function $\phi(T)$ approximately follows a logarithmic behavior, resembling the temperature dependence of χ near T_c . Moreover a clear jump appears at T_c , due to the change in the fractal dimension of the adsorbing set of sites of the substrate ($d_f = 1$ for $T < T_c$ and $d_f = 2$ for $T \geq T_c$) observed in the finite samples used in the simulations. This result

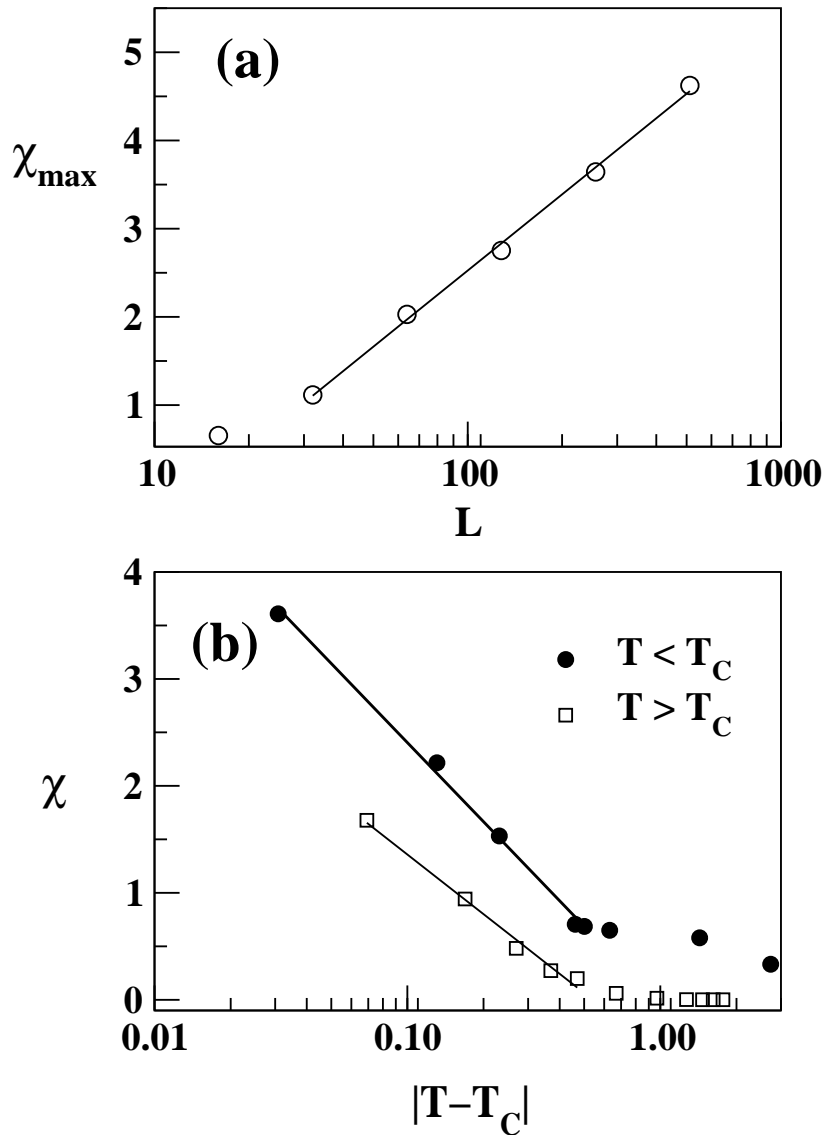


Figure 7: Data corresponding to the RSA of dimers on **BA**'s. (a) Linear-log plot of χ_{\max} versus L . (b) Linear-log plot of χ versus $|T - T_C|$ (in units of J) obtained using lattices of size $L = 256$. Both plots show that χ reflects the divergences of the specified heat of the underlying **BA**.

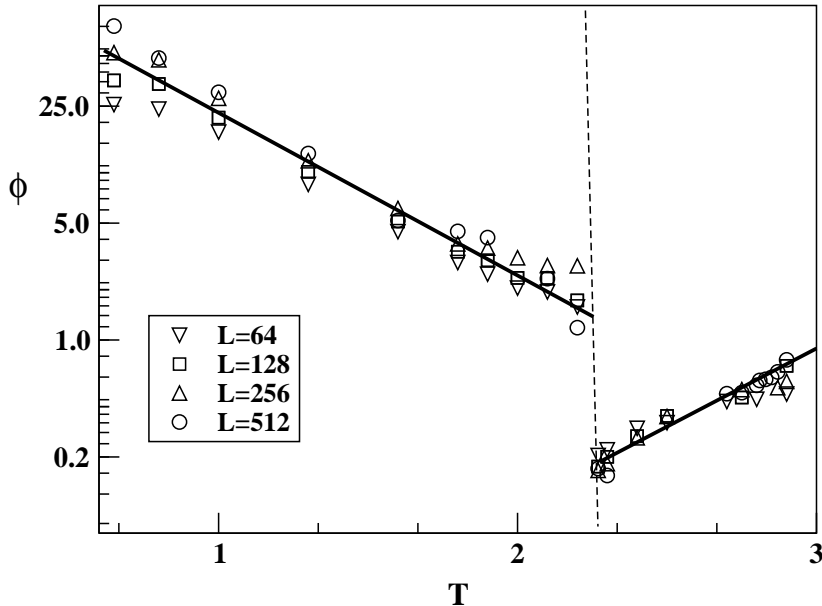


Figure 8: Plot of ϕ versus T (T in units of J), obtained using lattices of different size L . The jump observed in ϕ occurs at T_C (dashed line). The solid lines have been drawn to guide the eyes.

implies that the temperature dependence of the structure of the substrate prevails over that of the RSA process, and that the fluctuations due to substrate also prevails over those due to the RSA process (notice that $f(L) \rightarrow 0$ when $L \rightarrow \infty$).

5 Conclusions

In this paper the behavior of the fluctuations of the jamming coverage upon RSA process on homogeneous and nonhomogeneous substrates has been studied. Pointing the attention to the RSA process and applying the definition given by Eq. (8) in order to measure the fluctuations, we have shown both analytically and by means of numerical simulations, that the jamming fluctuations behaves as $\sigma_{\theta_J} \propto L^{-1/\nu_J}$, where ν_J is given by $\nu_J = \frac{2}{2D-d_f}$, D and d_f being the dimension of the lattice and that of the active sites where adsorption actually takes place, respectively. These results are suitable to describe systems characterized by a short-range correlation length of the RSA process, that may take place on both, homogeneous and nonhomogeneous substrate. From our derivation of Eq. (23) it follows that $\nu_J = 1$ for $D = 2$ and $d_f = 2$, in accordance with results published previously by various authors [8, 9, 15].

It should also be noticed that Eq. (23) allow us to measure the fractal dimension of the different adsorption sets where deposition takes place according to the specified adsorption rules. Summing up, our results not only point out that a careful treatment of the fluctuations of correlated processes is necessary in order to capture the desired physical behavior, but also provide a tool for the evaluation of fractal dimensions using RSA experiments.

Acknowledgments: This work was supported by CONICET, UNLP and ANPCyT (Argentina).

References

- [1] A. Patrykiewicz, S. Sokotowski and K. Binder, Surf. Sci. Rep. **37**, 207 (2000).
- [2] T. L. Einstein, *Chemistry and Physics of Solid Surfaces*, Vol. 4, Ed. R. Vanselow and R. Hove, Springer-Verlag, Berlin (1982).
- [3] W. H. Weinberg, Ann. Rev. Phys. Chem. **34**, 217 (1983).
- [4] R. S. Nord and J. W. Evans, J. Chem. Phys. **82**, 2795 (1985).
- [5] J. t. Terrell and R. S. Nord; Phys. Rev. A., **46**, 5260 (1992).
- [6] J. W. Evans, Rev. Mod. Phys., **65**, 1281 (1993).
- [7] J. J. Ramsden, J. Stat. Phys. **73**, 853 (1993).
- [8] N. Vandewalle, S. Galam and M. Kramer, Eur. Phys. J. B, **14**, 407 (2000).
- [9] G. Kondrat and A. Pekalski, Phys. Rev. E, **63**, 051108 (2001)
- [10] F. Rampf and E. V. Albano, Phys. Rev. E.,**66**, 061106 (2002).
- [11] *Fractals and Disordered Systems*, Eds. A. Bunde and S. Havlin. Springer-Verlag. Heidelberg, (1991).
- [12] *Fractals in Science*, Eds. A. Bunde and S. Havlin. Springer-Verlag. Heidelberg, (1994).
- [13] D. Stauffer and A. Aharony, *Introduction to the Percolation Theory*, Taylor and Francis, London, (1992) 2nd edition.
- [14] Notice that the occupation probability p , in the percolation framework, is equivalent to the coverage θ used within the terminology of RSA.
- [15] M. Nakamura, J. Phys. A, **19**, 2345 (1986).
- [16] Instead of using Eq. (8) one can also evaluate the fluctuations as $\langle \sigma_{\{Rsa\}} \rangle = \sum_{\lambda=1}^M \frac{\sigma_{\theta}^{(\lambda)}}{M}$. However, the relative difference between both, $\sigma_{\{Rsa\}}$ and $\langle \sigma_{\{Rsa\}} \rangle$, is negligible. In fact, evaluating $\frac{\sigma_{\{Rsa\}}}{\langle \sigma_{\{Rsa\}} \rangle} \approx (1 + \frac{1}{2}\epsilon^2)$, one has that ϵ is a second-order correction such as $\epsilon = \frac{\sigma_x}{x}$ with $x = \langle \sigma_{\{Rsa\}} \rangle$. We have checked that in our measurements one always has $\epsilon < 0.1$.
- [17] *The Monte Carlo Method in Condensed Matter Physics*, Ed. K. Binder. Springer-Verlag, Berlin, (1992).

- [18] J. M. Yeomans, *Statistical Mechanics of phase transitions*. Clarendon Press, Oxford, (1992).
- [19] *Nonequilibrium Statistical Mechanics in One Dimension* edited by V. Privman, Cambridge University Press Cambridge, 1997 and references therein
- [20] It can be demonstrated that $N_f \propto L^{\frac{2d_o-1}{d_o}}$, where N_f is the number of sites belonging to the diffusion front, $d_o = \frac{7}{4}$ is its fractal dimension of the inner perimeter of the front, L is the lateral extension of the front and L^{-1} is the density gradient along the sample.
- [21] B. Sapoval, M. Rosso and J. F. Gouyet. *J. Physique. Lett.* **46**, L49 (1985).
- [22] M. Rosso, J. F. Gouyet and B. Sapoval. *Phys. Rev. B.* **32**, 6053 (1985).
- [23] M. Rosso, J. F. Gouyet and B. Sapoval. *Phys. Rev. Lett.* **57**, 3195 (1986).
- [24] A. Memsouk, Y. Boughaleb, R. Nassif and H. Ennamiri. *Eur. Phys. J. B.* **17**, 137 (2000).
- [25] A. Hader, A. Memsouk and Y. Boughaleb. *Eur. Phys. J. B.* **17**, 137 (2000).
- [26] P. Grasberger. *J. Phys. A. (Math. and Gen.)*. **19**, 2675 (1986).
- [27] R. M. Ziff and B. Sapoval. *J. Phys. A. (Math. and Gen.)*. **19**, L1169 (1986).
- [28] H. E. Stanley, *Introduction to phase transitions and critical phenomena*. Oxford University Press, New York, (1971).